

Electronic Supplementary Information for PCCP article:

Theoretical Investigation of the Solid-Liquid Phase Transition in Protonated Water Clusters

Kseniia Korchagina, Aude Simon, Mathias Rapacioli, Fernand Spiegelman, Jean-Marc L'Hermite, Isabelle Braud, Sébastien Zamith, Jérôme Cuny

In the following electronic supplementary information, we first present the procedure to determine transition temperatures from the theoretical heat capacity curves discussed in the main manuscript and their convergence with respect to the constraining radius. We also present all the results obtained for $(\text{H}_2\text{O})_{23}\text{H}^+$ that are discussed in the main text but not directly presented for clarity. This includes: total and local O-O-O angle distributions, the distributions of oxygen rings, the intermittent and continuous HB correlation functions and the proton position distributions as a function of temperature. The $(\text{H}_2\text{O})_{23}\text{H}^+$ results are presented with those of $(\text{H}_2\text{O})_{20}\text{H}^+$, $(\text{H}_2\text{O})_{21}\text{H}^+$ and $(\text{H}_2\text{O})_{22}\text{H}^+$ to allow for a better comparison. Finally, the temperature dependence of the gyration radius of $(\text{H}_2\text{O})_{21}\text{H}^+$ is also discussed.

Contents

1	Convergence of the Heat Capacity Curves with respect to the Constraining Radius	S2
2	Extraction of Transition Temperature from Caloric Curves	S3
3	Temperature Evolution of the Total O-O-O Angle Distribution	S4
4	Temperature Evolution of the Local O-O-O Angle Distribution	S5
5	Temperature Evolution of the Distributions of Oxygen Rings	S6
6	Temperature Evolution of Radius of Gyration in $(\text{H}_2\text{O})_{21}\text{H}^+$	S7
7	Temperature Evolution of the HB Correlation Functions	S8
8	Temperature Evolution of the Proton Localization	S9

1 Convergence of the Heat Capacity Curves with respect to the Constraining Radius

Figure S1 presents the heat capacity curve of $(\text{H}_2\text{O})_{21}\text{H}^+$ obtained with three different constraining radii r_0 : 8, 10 and 12 Å. From those three curves, one sees that the transition temperature is hardly modified by the r_0 value. Nevertheless, a stronger impact is observed from the maximum of the heat capacity curve to higher temperatures which corresponds to a temperature range where evaporation starts to occur. For this latter, a visual analysis of the simulations shows that it starts to occur after 160 K. This is in line with the weak impact of the constraining radius below this temperature and a stronger impact after 170 K. A similar behaviour was previously reported by Douady *et al.* for $(\text{H}_2\text{O})_{20}$.¹ Those results confirm that a value of 8 Å for r_0 is well adapted in the present study.

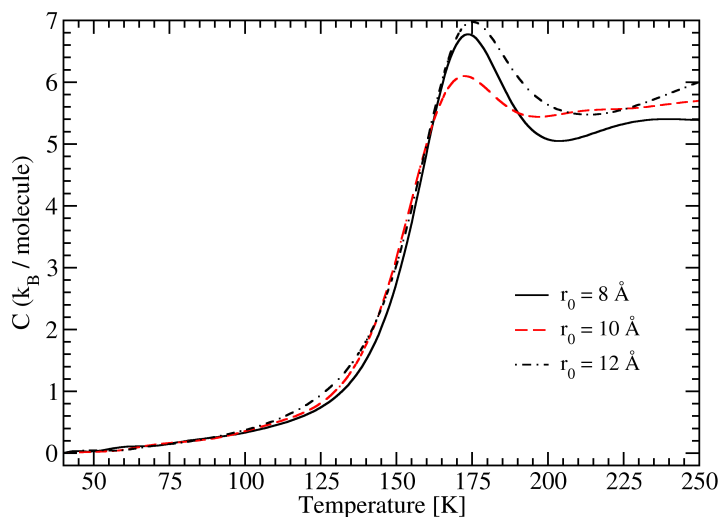


Figure S1: Heat capacity curves for $(\text{H}_2\text{O})_{21}\text{H}^+$ obtained for three different constraining radii.

2 Extraction of Transition Temperature from Caloric Curves

Figure S2 presents the procedure applied to extract the transition temperature from a theoretical caloric curve. It is worth pointing out that the same approach was used in the experimental study by Boulon *et al.*²

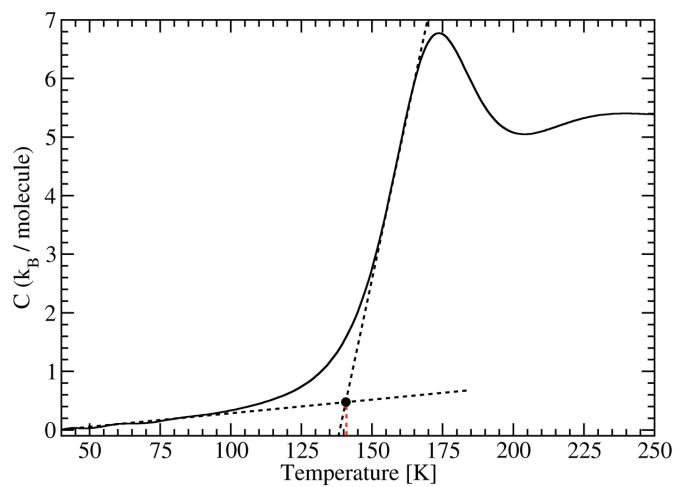


Figure S2: Scheme describing the determination of the transition temperature from a caloric curves. The theoretical curve obtained for $(\text{H}_2\text{O})_{21}\text{H}^+$ was used in this example.

3 Temperature Evolution of the Total O–O–O Angle Distribution

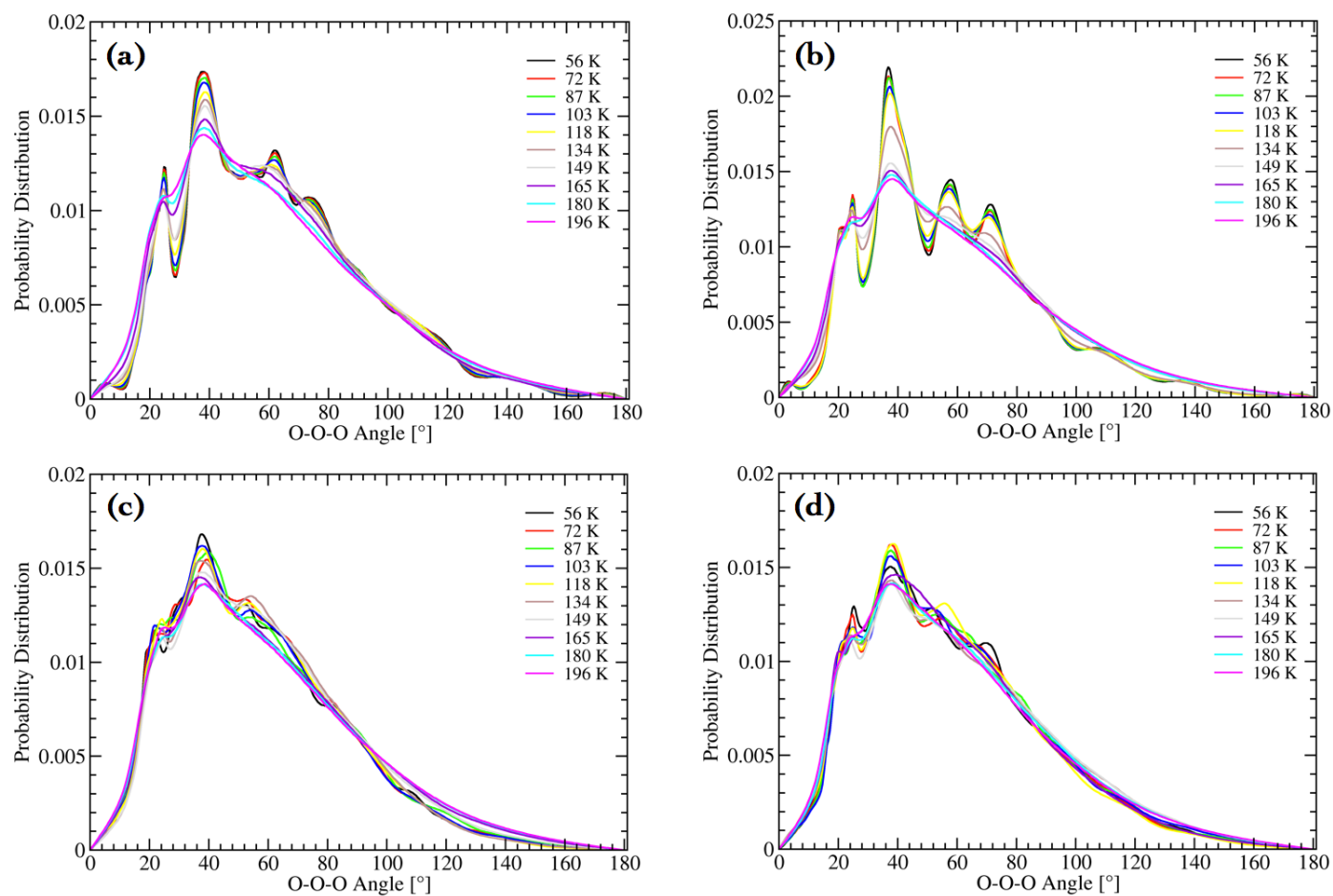


Figure S3: Temperature evolution of the total O–O–O angle distributions for (a) $(\text{H}_2\text{O})_{20}\text{H}^+$, (b) $(\text{H}_2\text{O})_{21}\text{H}^+$, (c) $(\text{H}_2\text{O})_{22}\text{H}^+$ and (d) $(\text{H}_2\text{O})_{23}\text{H}^+$.

4 Temperature Evolution of the Local O-O-O Angle Distribution

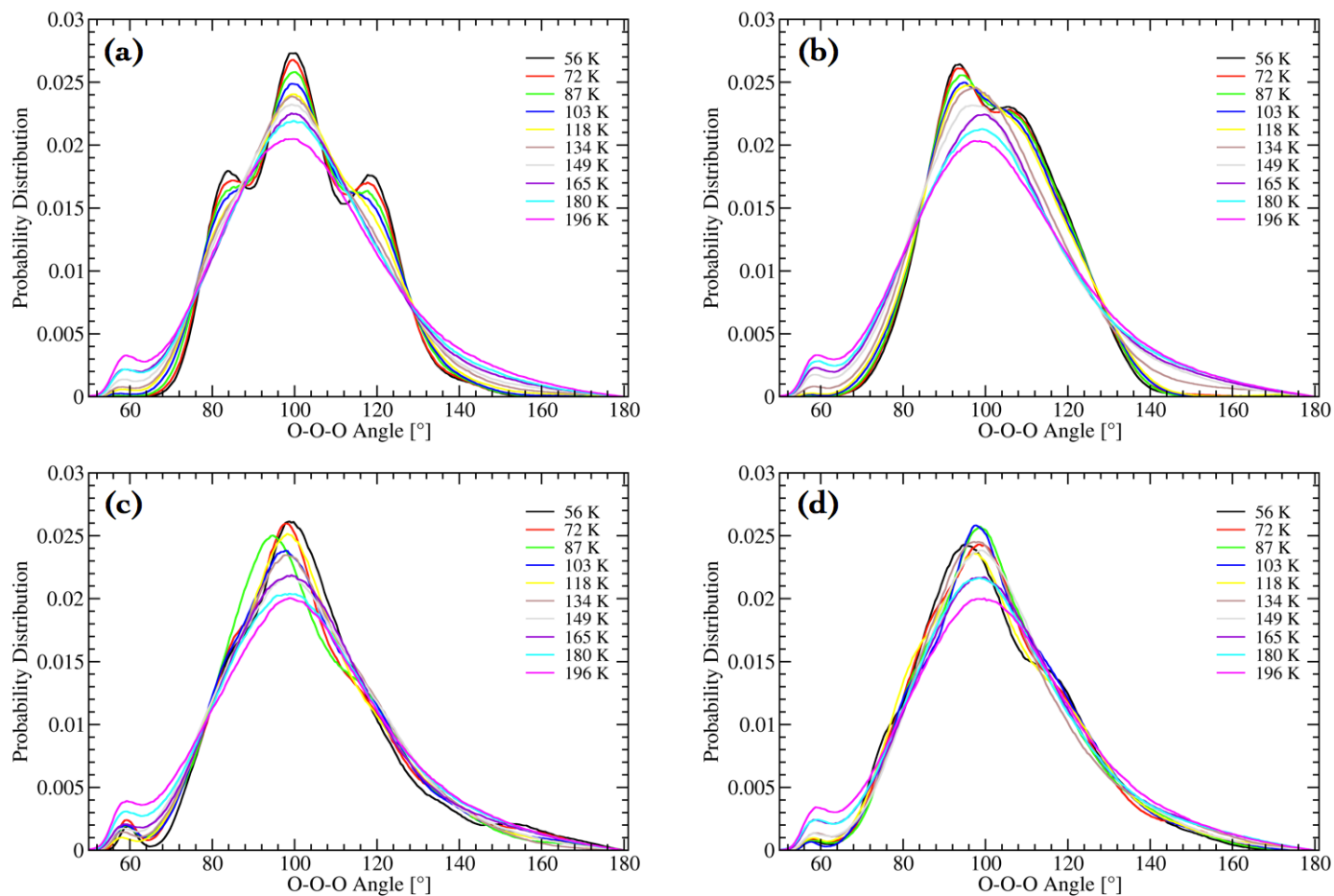


Figure S4: Temperature evolution of the local O-O-O angle distributions for (a) $(\text{H}_2\text{O})_{20}\text{H}^+$, (b) $(\text{H}_2\text{O})_{21}\text{H}^+$, (c) $(\text{H}_2\text{O})_{22}\text{H}^+$ and (d) $(\text{H}_2\text{O})_{23}\text{H}^+$.

5 Temperature Evolution of the Distributions of Oxygen Rings

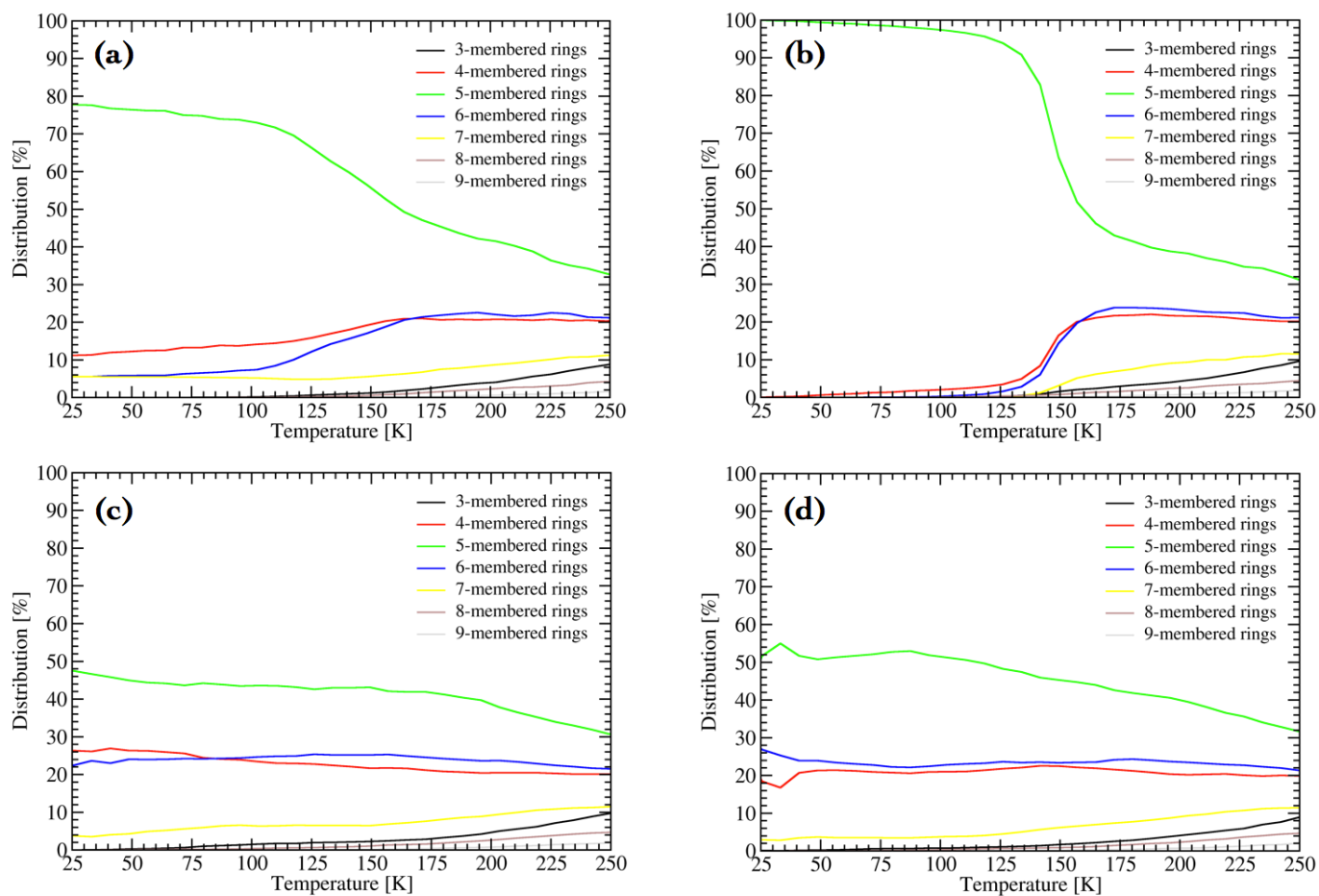


Figure S5: Temperature evolution of the distribution of oxygen rings within (a) $(\text{H}_2\text{O})_{20}\text{H}^+$, (b) $(\text{H}_2\text{O})_{21}\text{H}^+$, (c) $(\text{H}_2\text{O})_{22}\text{H}^+$ and (d) $(\text{H}_2\text{O})_{23}\text{H}^+$.

6 Temperature Evolution of Radius of Gyration in $(\text{H}_2\text{O})_{21}\text{H}^+$

Figure S6 displays the evolution of the gyration radius s^2 of $(\text{H}_2\text{O})_{21}\text{H}^+$ with respect to temperature. This curve was obtained by considering the oxygen atoms only. Figure S6 shows that s^2 is constant up to ~ 140 K, the transition temperature for this aggregate, and then, continuously increases. This reveals that the transition is associated with the opening of the dodecahedron structure and the loss of the low-temperature compact configuration. Kuo and Klein previously observed this transformation for the $(\text{H}_2\text{O})_n\text{H}^+$ $n=5-22$ species.³ They showed that aggregates with $n \geq 16$ undergo a transition from cage structures at low temperature to flower- and ring-type structures as temperature increases.

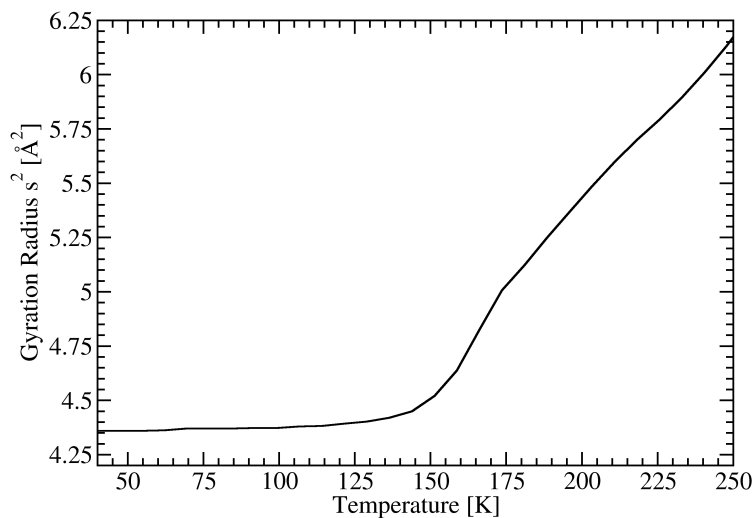


Figure S6: Radius of gyration (s^2) in $(\text{H}_2\text{O})_{21}\text{H}^+$ as a function of temperature.

7 Temperature Evolution of the HB Correlation Functions

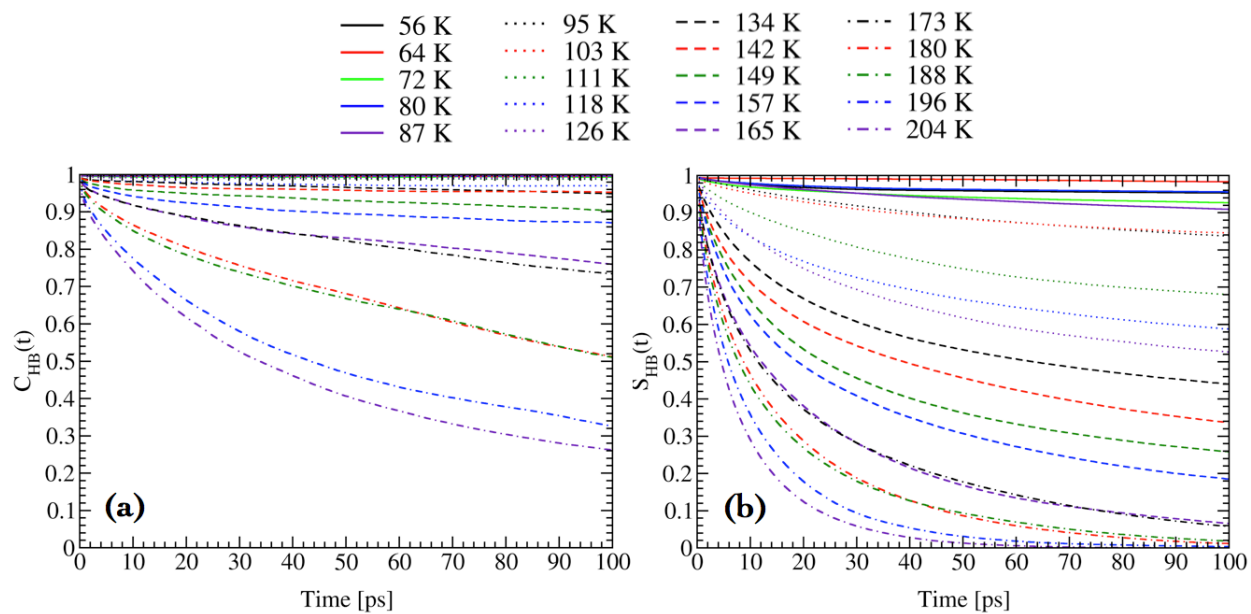


Figure S7: Intermittent HB correlation functions $C_{HB}(t)$ (a) and continuous HB correlation functions $S_{HB}(t)$ (b) for $(\text{H}_2\text{O})_{23}\text{H}^+$ as a function of the temperature.

8 Temperature Evolution of the Proton Localization

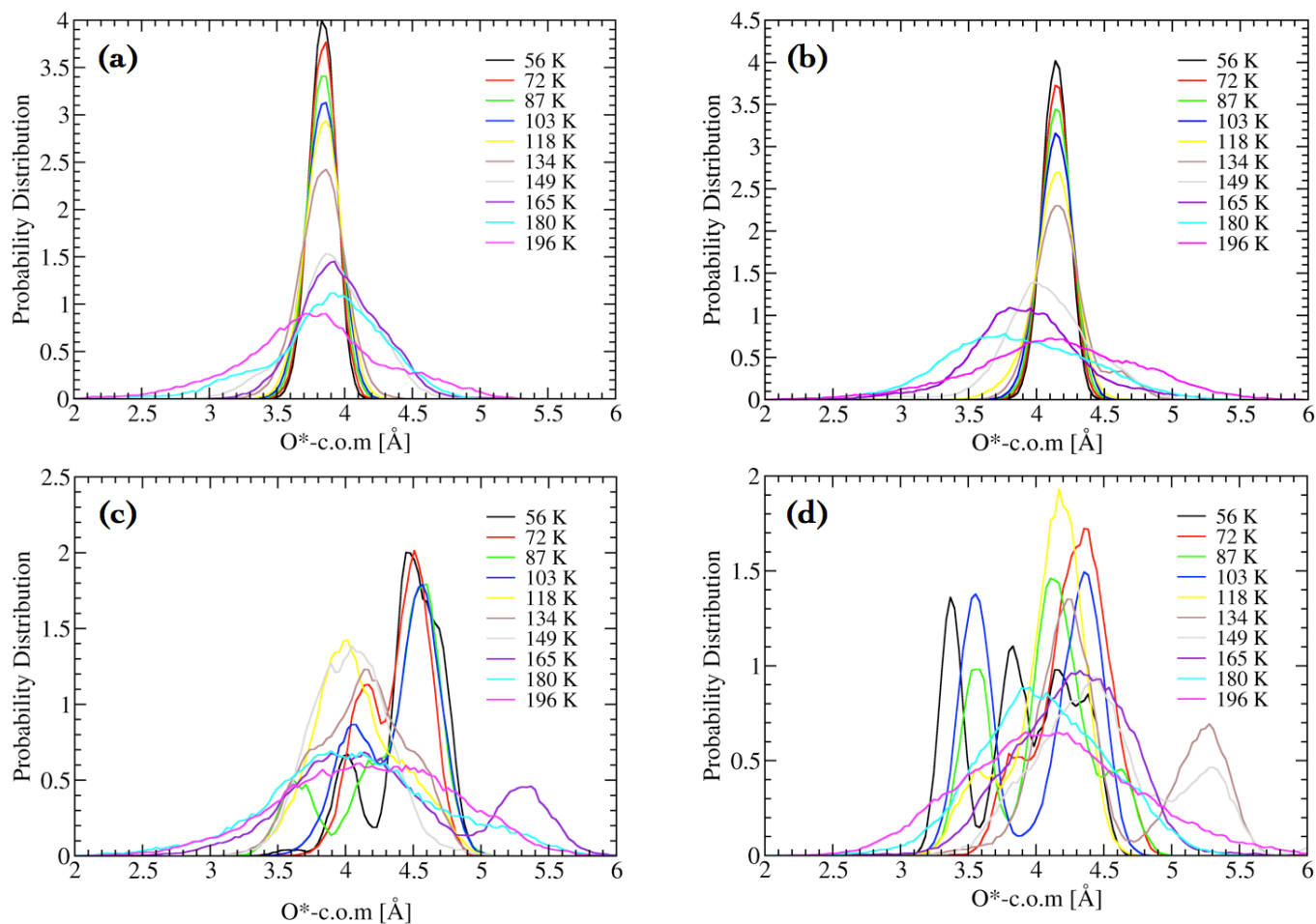


Figure S8: Temperature evolution of the distribution of distances between the oxygen-bearing excess proton and the center of mass of the cluster within (a) $(\text{H}_2\text{O})_{20}\text{H}^+$, (b) $(\text{H}_2\text{O})_{21}\text{H}^+$, (c) $(\text{H}_2\text{O})_{22}\text{H}^+$ and (d) $(\text{H}_2\text{O})_{23}\text{H}^+$.

References

- [1] J. Douady, F. Calvo and F. Spiegelman, *Eur. Phys. J. D*, 2009, **52**, 47–50.
- [2] J. Boulon, I. Braud, S. Zamith, P. Labastie and J.-M. L’Hermite, *J. Chem. Phys.*, 2014, **140**, 16435.
- [3] J.-L. Kuo and M. L. Klein, *J. Chem. Phys.*, 2005, **122**, 024516.